Neuron 49, 365–377, February 2, 2006 ©2006 Elsevier Inc. DOI 10.1016/j.neuron.2005.10.036

Runx1 Determines Nociceptive Sensory Neuron Phenotype and Is Required for Thermal and Neuropathic Pain

Chih-Li Chen,[1,5,6] Daniel C. Broom,[2,5,7] Yang Liu,[1,5] Joriene C. de Nooij,[3] Zhe Li,[4,8] Chuan Cen,[1] Omar Abdel Samad,[1] Thomas M. Jessell,[3] Clifford J. Woolf,[2] and Qiufu Ma[1,*]

[1] Dana-Farber Cancer Institute
and Department of Neurobiology
Harvard Medical School
1 Jimmy Fund Way
Boston, Massachusetts 02115

[2] Department of Anaesthesia and Critical Care
Massachusetts General Hospital
and Harvard Medical School
MGH-East
149 13th Street
Charlestown, Massachusetts 02129

[3] Howard Hughes Medical Institute
Department of Biochemistry and Molecular Biophysics
Center for Neurobiology and Behavior
Columbia University
New York, New York 10032

[4] Department of Biochemistry
Dartmouth Medical School
Hanover, New Hampshire 03755

Summary

In mammals, the perception of pain is initiated by the transduction of noxious stimuli through specialized ion channels and receptors expressed by nociceptive sensory neurons. The molecular mechanisms responsible for the specification of distinct sensory modality are, however, largely unknown. We show here that Runx1, a Runt domain transcription factor, is expressed in most nociceptors during embryonic development but in adult mice, becomes restricted to nociceptors marked by expression of the neurotrophin receptor Ret. In these neurons, Runx1 regulates the expression of many ion channels and receptors, including TRP class thermal receptors, Na^+-gated, ATP-gated, and H^+-gated channels, the opioid receptor MOR, and Mrgpr class G protein coupled receptors. Runx1 also controls the lamina-specific innervation pattern of nociceptive afferents in the spinal cord. Moreover, mice lacking *Runx1* exhibit specific defects in thermal and neuropathic pain. Thus, *Runx1* coordinates the phenotype of a large cohort of nociceptors, a finding with implications for pain therapy.

*Correspondence: qiufu_ma@dfci.harvard.edu

[5] These authors contributed equally to this work.

[6] Present address: School of Medicine, Fu-Jen Catholic University, Taipei, Taiwan.

[7] Present address: Neurogen Corporation, 35 Northeast Industrial Road, Branford, CT 06405.

[8] Present address: Children's Hospital, Division of Haematology/Oncology, 300 Longwood Avenue, Boston, MA 02115.

Introduction

In mammals, noxious peripheral stimuli are conveyed by nociceptors, a specialized group of primary sensory neurons with high stimulus thresholds and with cell bodies in the trigeminal and dorsal root ganglia (DRG) (Julius and Basbaum, 2001; Lewin and Moshourab, 2004; Perl, 1984; Tominaga and Caterina, 2004). Nociceptive sensory information is transmitted to the dorsal horn of the spinal cord where it is processed, relayed to the brain, and perceived as pain (Craig, 2003; Hunt and Mantyh, 2001; Light and Perl, 1979a, 1979b; Perl, 1998; Price et al., 2003). The sensitization of nociceptors under pathological conditions contributes to chronic pain, a major medical problem (Marchand et al., 2005; McMahon and Jones, 2004; Scholz and Woolf, 2002; Woolf, 2004).

At a molecular level, nociceptors express a diverse array of ion channels that transduce intense mechanical, thermal, or chemical stimuli into electrical activity (Hunt and Mantyh, 2001; Julius and Basbaum, 2001; Lewin et al., 2004; Patapoutian et al., 2003; Wang and Woolf, 2005; Wood, 2004). These channels and receptors are generally expressed in a partially overlapping or mutually exclusive fashion. For example, in the mouse DRG, the cold receptor TRPM8 (McKemy et al., 2002; Peier et al., 2002) and the heat/vanilloid receptor TRPV1 (Caterina et al., 1997) segregate into different classes of nociceptors (Story et al., 2003). Furthermore, a dozen Mrgpr/SNSR class G protein coupled receptors (GPCRs) are expressed in a largely mutually exclusive fashion, revealing a previously unrecognized diversity of nociceptors (Dong et al., 2001; Lembo et al., 2002; Zylka et al., 2003, 2005).

To date, the molecular logic that governs the generation of nociceptor cell diversity is poorly understood. However, several observations suggest a potential hierarchical control of nociceptive neuron development. All embryonic nociceptors initially express TrkA, a receptor for the nerve growth factor or NGF (Huang and Reichardt, 2001). During postnatal development, some nociceptors extinguish TrkA and activate Ret expression, a receptor for glial-cell-line-derived neurotrophic factor (GDNF) (Molliver et al., 1997). $TrkA^+$ and Ret^+ afferents terminate in distinct lamina and have been postulated to mediate inflammatory and neuropathic pain, respectively (Figure 1A) (Snider and McMahon, 1998). Consistent with this view, several ion channels and receptors are preferentially expressed in one of these two populations of nociceptors (Bradbury et al., 1998; Dong et al., 2001; Potrebic et al., 2003; Zylka et al., 2003). Understanding how nociceptors segregate into $TrkA^+$ and Ret^+ subclasses may therefore be an important step in unraveling the logic behind nociceptor diversity.

Several transcription factors have been shown to control the development of nociceptive sensory neurons. The neuronal determination gene *Neurogenin1* (*Ngn1*) is required for the formation of most nociceptors (Ma et al., 1999). The homeobox gene *Brn3a* and the zinc-finger gene *Klf7* are required for the expression of the high affinity nerve growth factor (NGF) receptor TrkA and the

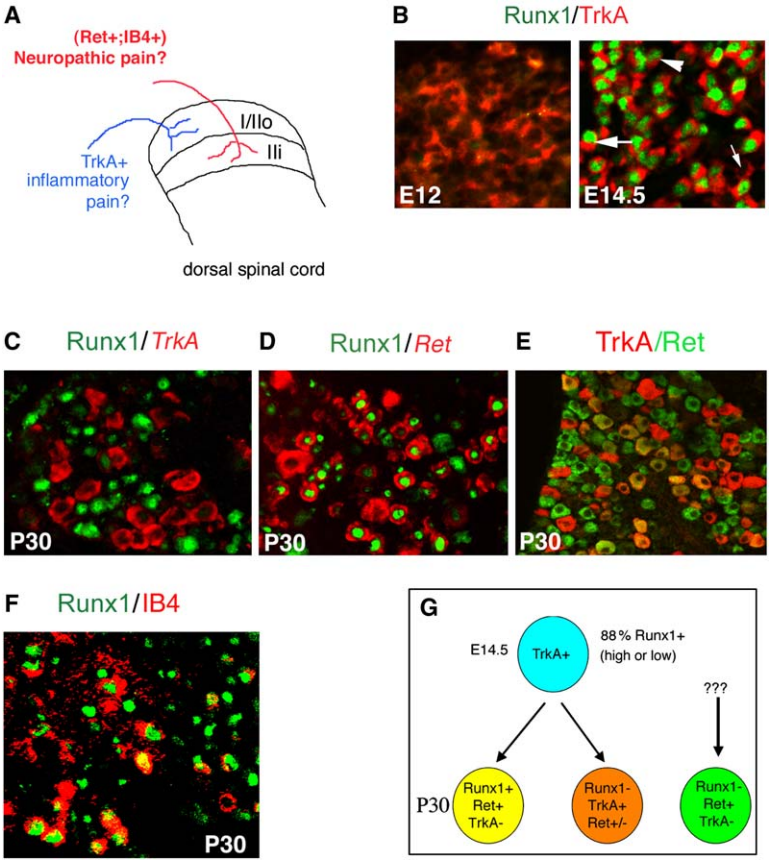

Figure 1. Runx1 Expression in the Developing and Adult DRG

(A) Differential expression of molecular markers and lamina-specific innervations in two classes of nociceptors. It has been postulated that IB4$^+$;Ret$^+$ (GDNF responsive) nociceptors might mediate neuropathic pain, whereas TrkA$^+$ nociceptors (NGF responsive) might be more critical for inflammatory pain (Snider and McMahon, 1998).

(B) Transverse sections through E12 and E14.5 DRG. Immunostaining of Runx1 (green) and TrkA (red) was performed. Note that at E12, no Runx1 expression is detected in TrkA$^+$ neurons. At E14.5, TrkA$^+$ neurons express a high level (large arrow), a low level (arrowhead), or none (small arrow) of Runx1. Runx1$^+$ neurons do not express *Ret* at this stage (data not shown).

(C and D) Transverse sections through P30 DRG showing absence of double staining of Runx1 protein (green) with *TrkA* mRNA (C, red) but a colabel of Runx1 (green) with *Ret* mRNA (D, red). Note that not all Ret$^+$ neurons coexpress Runx1 (D).

(E) Transverse sections through P30 DRG showing that some DRG neurons express TrkA alone (red), Ret alone (green), or both TrkA and Ret (partially yellow). Triple staining of TrkA, Ret, and Runx1 showed that some Ret$^+$ neurons express neither TrkA nor Runx1 (data not shown).

(F) In P30 DRG ~60% Runx1$^+$ neurons (green in nuclei) showed positive staining with the lectin IB4 (cell surface, red), a marker for a subset of Ret$^+$ nociceptors.

(G) Schematic indicating that Runx1 is expressed broadly in E14.5 TrkA$^+$ neurons; its expression persists in a subset of Ret$^+$ neurons but extinguishes in adult TrkA$^+$ neurons. TrkA expression also extinguishes in adult Runx1$^+$;Ret$^+$ neurons. The origin, identity, and function of Runx1$^-$;TrkA$^-$;Ret$^+$ cells remain obscure.

survival of nociceptors (Eng et al., 2004; Lei et al., 2005; Ma et al., 2003; McEvilly et al., 1996). The mammalian genome encodes three Runt domain transcription factors: Runx1/PEBP2αB/AML1, Runx2/PEBP2/AML3, and Runx3/PEBP2βC/AML2 (de Bruijn and Speck, 2004). These Runt proteins interact with a common cofactor CBFβ to control a variety of developmental processes (de Bruijn and Speck, 2004; Komori, 2005; Stein et al., 2004). Both *Runx1* and *Runx3* are expressed in the trigeminal and dorsal root ganglia (Inoue et al., 2002; Levanon et al., 2002; Theriault et al., 2004). *Runx3* is involved in the differentiation of proprioceptive sensory neurons (Inoue et al., 2002; Levanon et al., 2002), whereas *Runx1* expression appears to be restricted to nociceptors (Levanon et al., 2002; Theriault et al., 2004).

Despite this progress, transcription factors that are responsible for the segregation of TrkA$^+$ and Ret$^+$ nociceptors and/or the expression of nociceptive transduction ion channels have not yet been characterized. As a consequence, it has been unclear whether the specialized sensory modalities of individual classes of nociceptive sensory neurons are established independently or through a more coherent molecular program. In this study, we show that the persistent expression of Runx1 marks nociceptors that undergo the developmental TrkA to Ret transition, and in mice that selectively lack *Runx1* function in the peripheral nervous system, the TrkA to Ret transition is impaired. Moreover, we find that *Runx1* is required to activate or suppress the expression of a large cohort of nociceptive ion channels and sensory receptors. In addition, *Runx1* is required to target afferent projections to specific lamina in the dorsal spinal cord. Finally, behavioral analyses demonstrate specific deficits in thermal and neuropathic pain in *Runx1* deficient mice. These findings suggest that *Runx1* coordinates the phenotype of a large set of nociceptors.

Results

Persistent Runx1 Expression Marks a Subset of Ret$^+$ Nociceptors

To examine the involvement of Runx1 in sensory neuron differentiation, we first examined its expression profile during the developmental period that nociceptor subtypes emerge. TrkA expression is initiated at embryonic day 11.5 (E11.5) and detected robustly in E12 lumbar DRG neurons, whereas Runx1 expression is only first detected at E12.5 (Figure 1B and data not shown).

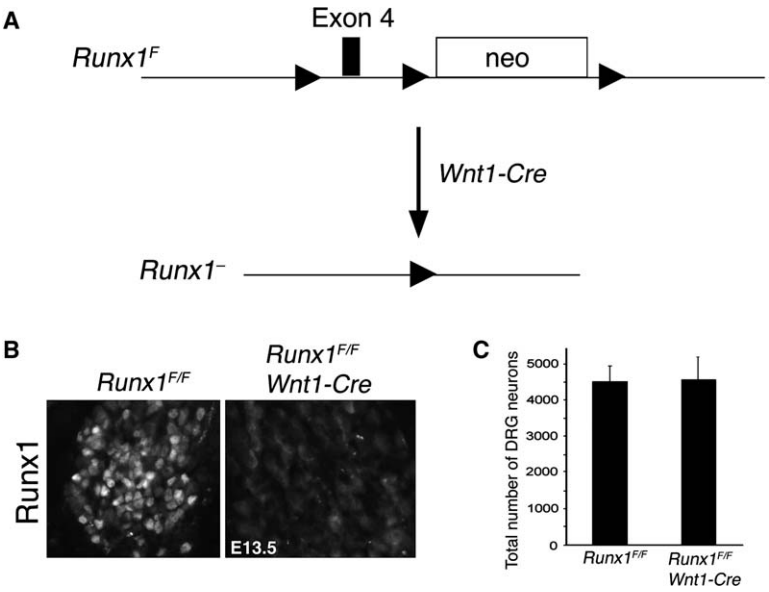

Figure 2. Conditional Knockout of *Runx1* in the DRG

(A) The schematics of the conditional allele. Exon 4, encoding part of the DNA binding Runt domain, is flanked with two *loxP* sequences (black triangles). Deletion of this exon is known to generate a null allele. The *neo* cassette in the intron region was also flanked with *loxP* sites. After crossing with *Wnt1-Cre* mice, the *neo* cassette and exon 4 were removed by Cre-mediated DNA recombination.

(B) Immunostaining of *Runx1* on sections through control $Runx1^{F/F}$ (left) and $Runx1^{F/F}$ *Wnt1-Cre* (right) DRG at E13.5. Note a nearly complete loss of Runx1 protein in $Runx1^{F/F}$ *Wnt1-Cre* DRG.

(C) Average (± SEM) neuronal numbers in the fifth lumbar (L5) DRG of $Runx1^{F/F}$ and $Runx1^{F/F}$ *Wnt1-Cre* mice are shown. No significant difference was detected ($p > 0.05$, with $p < 0.05$ considered as significant). Expression of the panneuronal marker *SCG10*, detected by in situ hybridization, was used to count neurons.

From E14.5 to postnatal day zero (P0), Runx1 expression is restricted to $TrkA^+$ neurons (Figure 1B), and about 88% of $TrkA^+$ neurons express either a high or low level of Runx1 (Figure 1B, large arrow versus arrowhead). By postnatal day (P) 6.5, an extinction of *TrkA* expression in some $Runx1^+$ neurons becomes apparent (data not shown). By P30, most $Runx1^+$ neurons no longer coexpress *TrkA* (Figure 1C) and instead colocalize with *Ret* (Figure 1D). However, not all Ret^+ neurons coexpress Runx1 (Figure 1D). Double staining of TrkA and Ret defines then three subclasses of adult DRG neurons: Ret^+, $TrkA^+$, and $TrkA^+Ret^+$ (Figure 1E). We conclude that persistent Runx1 expression marks those neurons that undergo a late developmental transition from a $TrkA^+$ to a Ret^+ status (Figure 1G). Runx1 expression is extinguished, however, in DRG neurons that remain $TrkA^+$ in the late postnatal period.

Generation of *Runx1* Conditional Knockout Mice

To examine the influence of *Runx1* on the differentiation of nociceptive sensory neurons, we examined the phenotype of conditional *Runx1* knockout mice. Mice carrying a *loxP*-based conditional *Runx1* allele (Growney et al., 2005) (referred here to as $Runx1^F$) (Figure 2A) were crossed with a *Wnt1-Cre* mouse strain that directs *Cre* expression in premigratory neural crest cells, including progenitors of DRG neurons (Jiang et al., 2000). In $Runx1^{F/F}$;*Wnt1-Cre* (for simplicity, $Runx1^{-/-}$) mice, there is no detectable expression of Runx1 in DRG neurons at E13.5 (Figure 2B) or in adult DRG (data not shown), suggesting a nearly complete penetration of Cre-mediated recombination. $Runx1^{-/-}$ mice are viable and fertile with no overt abnormalities. Moreover, DRG neuron numbers are similar in $Runx1^{-/-}$ and control $Runx1^{F/F}$ mice (Figure 2C), indicating that *Runx1* is not required for the genesis or survival of DRG neurons.

Impaired Transition from $TrkA^+$ to Ret^+ Nociceptors in $Runx1^{-/-}$ Mice

In $Runx1^{-/-}$ mice, we observe a dramatic change in the proportions of $TrkA^+$ and Ret^+ neurons (Figure 3). At P60, the percentage of $TrkA^+$ neurons in lumbar DRG is increased from 28% ± 3% in $Runx1^{F/F}$ control mice to 69% ± 6% in $Runx1^{-/-}$ mice ($p < 0.001$, with $p < 0.05$ considered as significant) (Figures 3A, 3B, and 3I), and conversely, the percentage of Ret^+ DRG neurons decreases from 69% ± 6% to 30% ± 2% ($p < 0.001$) (Figures 3C, 3D, and 3I). An incomplete loss of *Ret* is consistent with our finding that not all Ret^+ neurons coexpress Runx1 (Figure 1D).

The change in the proportions of $TrkA^+$ and Ret^+ neurons could result from a fate transformation from Ret^+ to $TrkA^+$ or a selective loss of Ret^+ neurons followed by a compensatory reduction in the death of $TrkA^+$ neurons. To distinguish between these two possibilities, we assessed the phenotype of neurons that label with the lectin IB4 in $Runx1^{-/-}$ DRG. In wild-type DRG, a subset of Ret^+ neurons colabels with IB4 and ~90% of $IB4^+$ neurons coexpress Runx1, whereas $TrkA^+$ neurons rarely label with IB4 (Figures 1F, 3E, and 3G) (Molliver et al., 1997). The percentage of IB4-labeled neurons in lumbar DRG is unchanged between $Runx1^{-/-}$ mice (30% ± 4%) and control mice (31% ± 5%) ($p = 0.42$), but most $IB4^+$ neurons no longer express *Ret* and instead express TrkA in $Runx1^{-/-}$ mice (Figures 3F and 3H). These findings suggest that Runx1 is required for the developmental transition from a $TrkA^+$ to a Ret^+ phenotype, by suppressing *TrkA* and promoting *Ret* expression (summarized in Figure 3J).

Loss of Nociceptive Ion Channels and Sensory Receptors in $Runx1^{-/-}$ Mice

The expression of high threshold ion channels defines the specialized peripheral receptive properties of nociceptor subclasses (Hunt and Mantyh, 2001; Jordt et al., 2003; Julius and Basbaum, 2001; Lewin et al., 2004; Patapoutian et al., 2003; Wood, 2004). To determine if *Runx1* is required for the specification of different transduction phenotypes, we compared the expression of nociceptive ion channels and sensory receptors in $Runx1^{-/-}$ and control $Runx1^{F/F}$ mice.

TRP class ion channels transduce a wide range of thermal stimuli, including noxious cold or heat (Jordt et al., 2003; Patapoutian et al., 2003; Wang and Woolf,

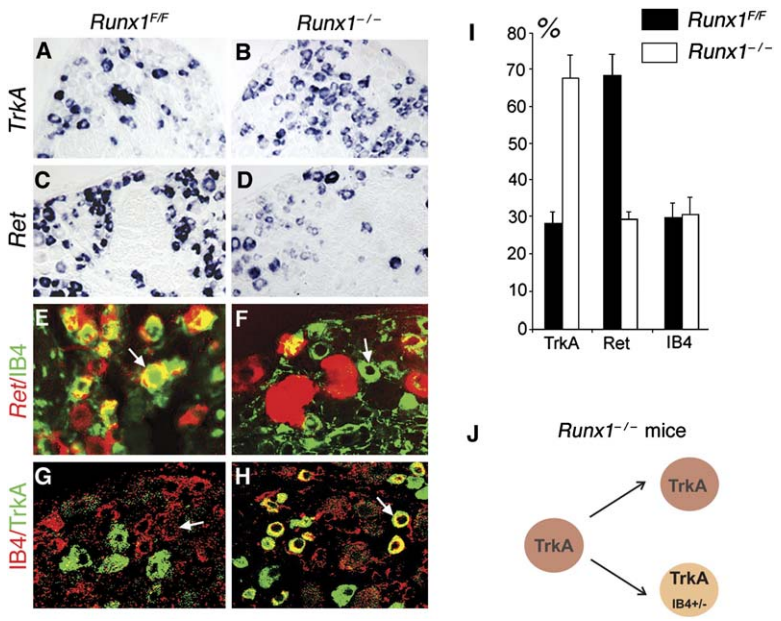

Figure 3. Transformation of Ret$^+$ into TrkA$^+$ Nociceptors in *Runx1*$^{-/-}$ Mice

Transverse sections through adult DRG (A–H). (A-D) In situ hybridization with *TrkA* or *Ret* probes. (E and F) Double labeling for IB4 binding (green) and *Ret* mRNA (red) on adult DRG sections. Note that in control *Runx1*$^{F/F}$ DRG, IB4$^+$ cells coexpress *Ret* (E, arrow), but in adult *Runx1*$^{-/-}$ DRG, most IB4$^+$ neurons lose *Ret* expression (F, arrow). (G and H) Double labeling for IB4 binding (red) and TrkA protein (green) on adult DRG sections. IB4$^+$ cells do not express TrkA in control *Runx1*$^{F/F}$ DRG, but they do in *Runx1*$^{-/-}$ DRG. (I) Average (± SEM) percentages of DRG neurons expressing the molecular markers in control *Runx1*$^{F/F}$ and *Runx1*$^{-/-}$ mice are shown. (J) Schematic of the transformation of prospective Ret$^+$ into TrkA$^+$ nociceptors in mutants (in comparison with the situation occurring in wild-type DRG, Figure 1G). In *Runx1*$^{-/-}$ mice, all nociceptors retain TrkA expression, although the "transformed" cells retain IB4 staining.

2005). Expression of two putative cold receptors *TRPM8* and *TRPA1* is first detected at E16.5 in wild-type DRG (data not shown); however, their expression is absent at every stage examined in *Runx1*$^{-/-}$ mice (E16.5, P0, P7, P30, and P60) (Figure 4A and see also below Figure 5; data not shown), indicating that *Runx1* is required to initiate the expression of these transduction molecules. Expression of the heat receptors *TRPV1* and *TRPV2,* as well as *TRPC3,* is also eliminated or markedly reduced in adult *Runx1*$^{-/-}$ DRG (Figure 4A). The percentage of L4 and L5 DRG neurons expressing a high level of *TRPV1* is reduced from 2.6% ± 0.5% to none ($p < 0.01$) and *TRPV2* (high level) from 25% ± 3% to 6% ± 1% ($p < 0.001$) (Figure 4A). However, the number of neurons that express an intermediate level of *TRPV1* is not reduced (Figure 4A; data not shown), implying that Runx1 is required for elevated but not basal levels of expression of this heat receptor. The *Mrgpr* genes (*Mrg/SNSR*) encode a dozen GPCRs that are expressed exclusively in Ret$^+$;IB4$^+$ nociceptors (Dong et al., 2001; Lembo et al., 2002; Zylka et al., 2003; Zylka et al., 2005), and activation of *Mrgprc/SNSR1* in rat causes hypersensitivity to heat and mechanical stimuli (Grazzini et al., 2004). In *Runx1*$^{-/-}$ mutants, expression of *Mrgprd*, *Mrgprb4*, and *Mrgprb5* is absent at every stage examined (Figure 4B), whereas expression of other *Mrgpr* genes, including *Mrgpra1-a8* and *Mrgprc,* is markedly reduced in *Runx1*$^{-/-}$ DRG (C.-L.C. and Q.M., unpublished data).

ATP released from damaged tissue evokes a painful response by activating ATP-gated channels (P2Xs) (Wood, 2004). The percentage of neurons expressing the nociceptor-specific *P2X3* channel (Chen et al., 1995) is markedly reduced in *Runx1*$^{-/-}$ DRG (from 32% ± 3% to 13% ± 2%; $p < 0.001$) (Figure 4D). In addition, high-level expression of the tetrodotoxin-resistant Na$^+$ channel gene *Nav1.9/SNS2*, which contributes to nociceptor membrane excitability (Dib-Hajj et al., 1998; Wood et al., 2004), is virtually eliminated, from 28% ± 3% in control DRG to less than 0.1% in *Runx1*$^{-/-}$ DRG ($p < 0.001$) (Figure 4C). Furthermore, at P30, Runx1 protein is detected in the majority of wild-type DRG neurons that express *TRPC3*, *P2X3*, *Nav1.9*, or *Mrgprd* (Figure 4E), suggesting that Runx1 may control the expression of these channels in a cell-autonomous manner.

In contrast, expression of *ASIC*, encoding a proton-gated ion channel (Waldmann and Lazdunski, 1998), is unchanged (19% ± 1% in *Runx1*$^{F/F}$ control mice versus 18% ± 1% in *Runx1*$^{-/-}$ mice; $p > 0.05$) (see below Figures 5C and 5D). Likewise, no obvious reduction is observed in the expression of another TTX-resistant channel *Nav1.8/SNS*, which is expressed in a majority of nociceptors in mouse DRG (Agarwal et al., 2004) (data not shown). We conclude that *Runx1* coordinates the expression of many but not all nociceptive transduction ion channels and receptors, ranging from thermal receptors, ATP-gated and Na$^+$-gated channels, as well as a large family of GPCRs.

Derepression in *Runx1*$^{-/-}$ DRG Neurons

In *Runx1*$^{-/-}$ DRG, presumptive Ret$^+$ neurons transform into TrkA$^+$ neurons. This led us to examine if the expression of genes, which in wild-type DRG are preferentially associated with a TrkA$^+$ identity, is also affected in *Runx1* mutants. Most adult TrkA$^+$ neurons are peptidergic and express the genes encoding the precursors for the neuropeptides Substance P (SP) and Calcitonin Gene Related Peptide (CGRP) (Snider and McMahon, 1998). From E16.5 to P30 in wild-type DRG, CGRP$^+$ neurons either do not express or express a low level of Runx1 (Figure 5A). In *Runx1*$^{-/-}$ adult mice, however, there is a marked increase in the percentage of DRG neurons expressing *CGRP*, from 32% ± 2% to 64% ± 2% ($p < 0.001$) (Figures 5B and 5D). *SP*$^+$ neurons also shows a significant, albeit more modest, increase from 32% ± 4% to 43% ± 2% ($p < 0.0001$) (Figures 5B and 5D). The expansion of *CGRP* in *Runx1*$^{-/-}$ mice is also apparent by the detection of *CGRP* expression in IB4$^+$ neurons (Figure 5B), which is only very rarely observed in wild-type DRG (Figure 5B). Together, these findings suggest

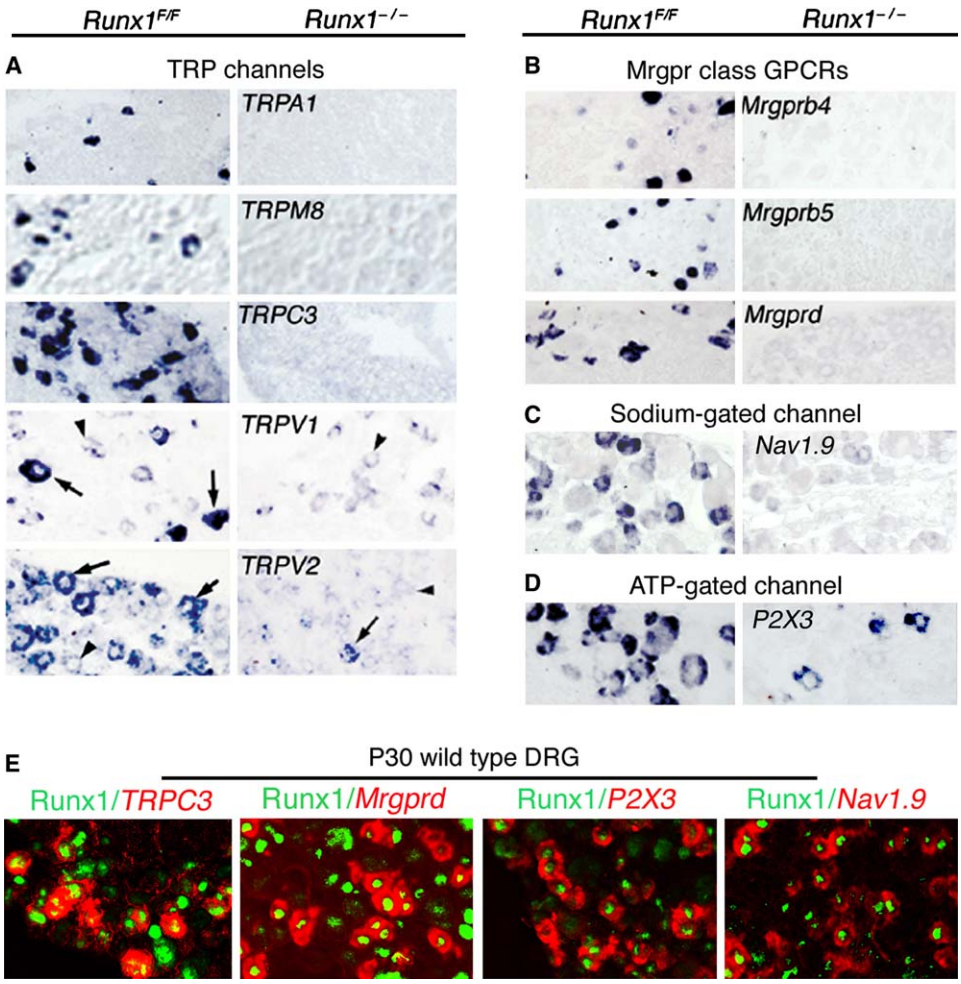

Figure 4. Regulation of Nociceptive Ion Channels and Sensory Receptors by Runx1

(A–D) Sections through adult control *Runx1*$^{F/F}$ and *Runx1*$^{-/-}$ DRG and in situ hybridization performed with indicated probes. Note the loss or marked reduction of diverse ion channels and receptors in *Runx1*$^{-/-}$ mice. Note a selective reduction of high-level (arrows) but not the intermediate expression (arrowheads) of *TRPV1* or *TRPV2*.

(E) Double labeling of Runx1 protein (green) and indicated probes (red) on adult wild-type P30 DRG sections. Note that Runx1 was expressed in the majority of neurons expressing *TRPC3*, *Mrgprd*, *P2X3*, or *Nav1.9/SNS2* (red). Runx1 expression is, however, not detected in a small fraction of *P2X3*$^{+}$, *Mrgprd*$^{+}$, or *Nav1.9*$^{+}$ neurons.

that in absence of *Runx1*, prospective nonpeptidergic nociceptors develop into CGRP^{+} peptidergic neurons.

The DRG acid-sensing channel DRASIC and the mu-class opioid receptor are associated preferentially with peptidergic identity (Li et al., 1998; Price et al., 2001). Consistently, in adult wild-type DRG Runx1^{+} neurons do not express *DRASIC* (Figure 5A). In *Runx1*$^{-/-}$ adult mice, there is, however, a marked increase in the percentage of DRG neurons expressing *MOR* (from 33% ± 2% to 63% ± 3%; $p < 0.001$) or *DRASIC* (from 22% ± 2% to 71% ± 5%; $p < 0.001$) (Figures 5C and 5D). Thus, within presumptive Ret^{+} neurons, *Runx1* is required to suppress the expression of a set of molecules normally associated with a TrkA identity (summarized in Figure 5E).

Runx1 Activates Expression of Some Ion Channels before It Acts to Switch off *TrkA* or Activate *Ret*

Runx1 is required to regulate the expression of both neurotrophin receptors and nociceptive ion channels (Figures 3–5). To determine if the loss/expansion of ion channels is caused by a change in neurotrophin-receptor signaling, we examined when Runx1 exerts these two activities. Expression of *TRPM8* and *Mrgprd* is first detected at E16.5 in wild-type DRG (Figures 6A and 6C; data not shown), and this expression is eliminated in *Runx1*$^{-/-}$ DRG at E16.5 (Figures 6B and 6D). A marked reduction of expression of *TRPV1* and *TRPA1* is also observed at P0 in *Runx1*$^{-/-}$ DRG (data not shown). However, at every embryonic or neonatal stage examined (E14.5, E17, and P0), nearly all Runx1^{+} neurons in wild-type DRG express TrkA (Figure 6E; data not shown). This suggests that Runx1 is required to activate channel/receptor expression at prenatal/neonatal stages before it acts to switch off TrkA expression at postnatal stages. By E17, Ret expression becomes apparent in a subpopulation of Runx1^{+} neurons (Figure 6F). At this stage, however, *TRPM8*$^{+}$ neurons do not coexpress Ret (Figures 6G–6I), suggesting that initiation of *TRPM8* expression is independent of Ret-mediated signaling.

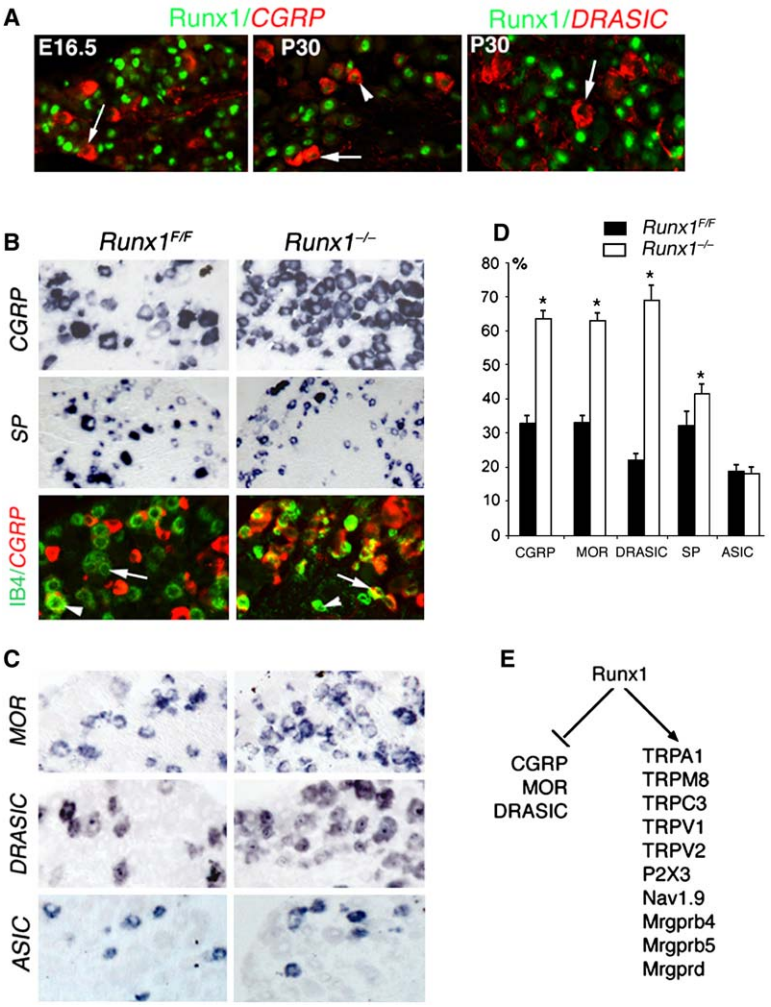

Figure 5. Derepression in *Runx1*$^{-/-}$ Mice

(A) Double labeling of Runx1 protein (green) and CGRP and *DRASIC* mRNA (red) on E16.5 or P30 DRG sections. Runx1^{+} neurons do not express CGRP at E16.5 or *DRASIC* at P30 (arrows), but some CGRP^{+} neurons express a low level of Runx1 at P30 (arrowhead).

(B, top, and C) In situ hybridization was performed on sections through adult wild-type and *Runx1*$^{-/-}$ DRG with indicated probes. (B, bottom) Double staining of *CGRP* mRNA (red) and IB4 binding (green). Most IB4^{+} neurons in control *Runx1*$^{F/F}$ P30 DRG do not express *CGRP* (arrow, left), although a small number of IB4^{+} neurons do (arrowhead, left). In *Runx1*$^{-/-}$ DRG, many IB4^{+} neurons now coexpress *CGRP* (right, arrow), although some mutant IB4^{+} neurons still lack *CGRP* (right, arrowhead).

(D) Average (± SEM) percentages of DRG neurons expressing the molecular markers in wild type and *Runx1*$^{-/-}$ mice are shown (asterisk, t test, $p < 0.001$).

(E) Runx1 activates and suppresses two separate groups of neuropetides, ion channels and sensory receptors.

Thus, the loss of many nociceptive ion channels in *Runx1*$^{-/-}$ DRG neurons is unlikely to be explained solely by the loss of *Ret* or the gain of *TrkA* expression, which in turn implies a more direct function for Runx1 in controlling the expression of these channels and receptors.

Central Afferent Targeting Is Impaired in *Runx1* Mutants

The precision in processing sensory information demands coordination between the specification of sensory modality and afferent central target selection. To determine if *Runx1* coordinates these two developmental processes, we examined afferent projections in the dorsal spinal cords of wild-type and *Runx1*$^{-/-}$ mice. In wild-type mice, IB4^{+} (Ret^{+}) afferents project predominantly to inner lamina II (IIi) (Figures 7A and 7G, arrows and Figure 7Q), whereas CGRP^{+} and SP^{+} peptidergic afferents (TrkA^{+}) predominantly project to lamina I and outer layer II (IIo) (Figures 7C, 7G, and 7K, arrowheads) and, to a lesser extent, to lamina IIi (Figures 7C, 7G, and 7K, arrows) (Snider and McMahon, 1998). In *Runx1*$^{-/-}$ mice, IB4^{+}, CGRP^{+}, and SP^{+} afferents all reach the dorsal horn (Figures 7B, 7D, and 7J), suggesting that initial axon pathfinding from the DRG to the spinal cord is independent of *Runx1*. However, double labeling of IB4 and CGRP or SP clearly shows a shift in IB4^{+} afferent innervation from the more ventral lamina to the most dorsal lamina of the dorsal horn (Figure 7H versus Figure 7G), whereas CGRP^{+} afferents (Figures 7D and 7H versus Figure 7C and 7G) and SP^{+} afferents (Figures 7J and 7L versus Figures 7I and 7K) still project predominantly to the most superficial lamina. The dorsal shift in IB4^{+} afferent innervation is also supported by the double labeling of IB4 and PKC-γ (Figures 7M–7P). In wild-type mice, IB4^{+} afferents terminate in the lamina exactly abutting the territory enriched with PKC-γ-positive neuronal cell bodies and processes (Figures 7M and 7O), but in *Runx1*$^{-/-}$ mice, the density of IB4^{+} afferents in this area is much reduced (Figures 7N and 7P versus Figures 7M and 7O, arrows).

In the dorsal horn of *Runx1*$^{-/-}$ mice, a subset of IB4^{+} afferents costains with CGRP (Figure 7H, arrow) and to a lesser extent with SP (Figure 7L, arrow), something rarely seen in wild-type mice (Figures 7G and 7K). This difference in colabeling with CGRP and SP is consistent with their dramatic (CGRP) and modest (SP) derepression in *Runx1*$^{-/-}$ IB4^{+} neurons (Figure 5). However, within the superficial dorsal lamina of *Runx1* mutant mice, some afferents express only CGRP or SP and do not label with IB4 (Figures 7H and 7L, arrowheads). This suggests that endogenous peptidergic afferents project normally in *Runx1*$^{-/-}$ mice. We conclude that a loss of

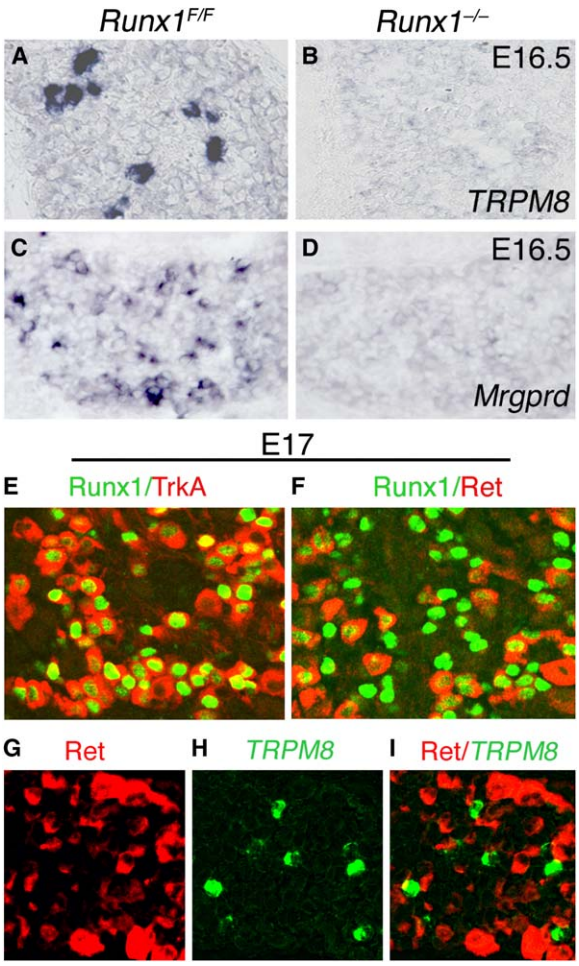

Figure 6. Runx1 Is Required to Activate Ion-Channel/Receptor Expression before It Controls Neurotrophin-Receptor Expression

(A–D) In situ hybridization on sections through E16.5 control *Runx1*$^{F/F}$ and *Runx1*$^{-/-}$ DRG.

(E and F) Double immunostaining of Runx1 protein (green) with TrkA protein (E, red) or Ret protein (F, red) in E17 wild-type DRG. Note effectively all Runx1^{+} neurons coexpress TrkA at this stage (E), but only a subpopulation of Runx1^{+} neurons express Ret (F).

(G–I) Double staining of *TRPM8* mRNA (green) and Ret protein (red) showed a lack of Ret expression in *TRPM8*$^{+}$ neurons in E17 DRG.

Runx1 appears to specifically perturb the laminar target selection of IB4^{+} afferents (summarized in Figures 7Q and 7R).

Deficits in Thermal and Neuropathic Pain

To examine if the molecular and anatomical defects in *Runx1*$^{-/-}$ mice are accompanied by alterations in behavioral responses to noxious stimuli, we assayed acute responses to noxious thermal and mechanical stimuli, as well as neuropathic and inflammatory pain sensitivity.

Runx1 mutants exhibit a significantly delayed reaction time to a noxious heat stimulus (50°C, 52°C, and 55°C hot plate) that is most evident at the lowest stimulus temperature (Figures 8A and 8B; data not shown). There is also a markedly diminished response to a cold stimulus (acetone evaporation) by *Runx1*$^{-/-}$ mice (Figure 8C). TRPV1 also serves as the receptor for capsaicin, the pungent ingredient in chili pepper (Jordt et al., 2003). In agreement with the loss of high-level expression of *TRPV1*, capsaicin-induced pain responses, as indicated by paw licking, flinching, and foot withdrawal (Caterina et al., 2000), are significantly reduced in *Runx1*$^{-/-}$ mice (Figure 8D). In marked contrast, we detected no change in the sensitivity of *Runx1*$^{-/-}$ mice to threshold mechanical noxious stimuli or to suprathreshold pinprick stimuli (Figures 8E and 8F), indicating that mechanical pain is not grossly altered by the loss of Runx1 function. These findings establish a specific requirement for Runx1 activity in sensory neurons for the detection of acute thermal, but not mechanical, noxious stimuli.

Neuropathic pain represents a heightened pain sensitivity induced by peripheral nerve injury, in which normally innocuous tactile stimuli can evoke pain or pain-like withdrawal response, a phenomenon termed mechanical allodynia (Woolf, 2004). We used the spared nerve injury model (SNI) (Decosterd and Woolf, 2000) to assess if neuropathic pain is affected in *Runx1*$^{-/-}$ mice. In control *Runx1*$^{F/F}$ mice, nerve injury induces mechanical allodynia, indicated by a substantial lowering of the paw withdrawal threshold (ANOVA interaction: $F[8,80] = 3.14$, $p < 0.01$) (Figure 8G). After SNI in *Runx1*$^{-/-}$ mice no change in paw withdrawal threshold is detected ($p > 0.05$), indicating an absence of mechanical allodynia. Thus, *Runx1* function is necessary for the manifestation of neuropathic pain responses.

Inflammatory pain occurs in response to peripheral tissue inflammation. We assessed if Runx1 function is involved in establishment of inflammatory pain responses by monitoring mechanical allodynia after intraplantar injection of complete Freund's adjuvant (CFA). CFA-induced inflammation occurred normally, as indicated by the swelling of the entire feet and hind legs in both *Runx1*$^{-/-}$ and control *Runx1*$^{F/F}$ mice (for quantitative data, see Experimental Procedures). However, although mechanical allodynia was still induced in the inflamed hindpaw, the degree of allodynia is significantly less in *Runx1*$^{-/-}$ than in control *Runx1*$^{F/F}$ mice (ANOVA interaction: $F[1,21] = 23.556$, $p < 0.001$) (Figure 8H). Runx1 may therefore have a role, albeit relatively minor, in the development of inflammatory pain.

Discussion

Roles of Runx1 in the Specification of TrkA^{+} and Ret^{+} Nociceptor Cell Fates

Three lines of evidence suggest that Runx1 function is required for the proper segregation of Ret^{+} and TrkA^{+} nociceptors. First, persistent expression of Runx1 marks those neurons that extinguish TrkA and switch on Ret, and a loss of *Runx1* in DRG sensory neurons results in a reduction in Ret^{+} neurons and a reciprocal increase in TrkA^{+} neurons. Second, many genes that are expressed in Ret^{+};IB4^{+} neurons, including *P2X3* and *Mrgpr* class GPCR genes (Bradbury et al., 1998; Dong et al., 2001; Zylka et al., 2003), are eliminated in *Runx1*$^{-/-}$ mice, whereas others preferentially expressed in TrkA^{+} neurons, including *CGRP*, *DRASIC*, and *MOR* (Li et al., 1998; Price et al., 2001), are expanded. Third, in wild-type mice, IB4^{+} (Ret^{+}) afferents project to the deep lamina of the dorsal horn, whereas in *Runx1*$^{-/-}$ mice, IB4^{+} afferents project to the most superficial lamina, which normally are only innervated by TrkA^{+} peptidergic

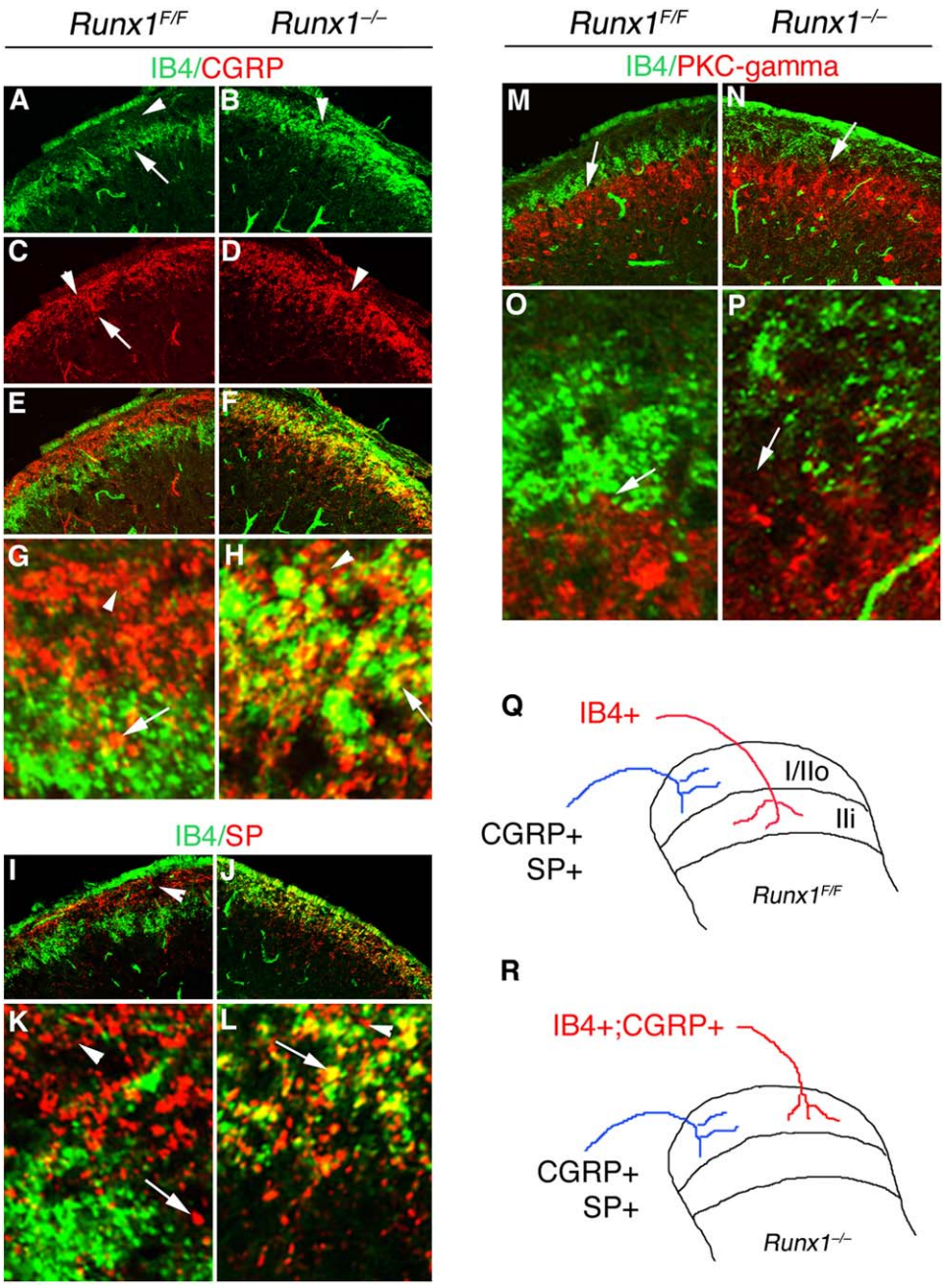

Figure 7. Afferent Central Target Selection in the Dorsal Horn Was Impaired in *Runx1*$^{-/-}$ Mice

Double staining of IB4 (A, B, and E–P, green) plus CGRP (C–H, red), SP (I–L, red), or PKC-γ (M–P, red) on P30 dorsal horn sections. (E) and (F) are the merged images shown in (A) – (D). (G), (H), (K), (L), (O), and (P) represent a higher magnification. (Q and R) Schematics showing the change of lamina-specific innervation of IB4$^+$ afferents: from a deep lamina in wild-type dorsal horn (Q, red) to a more superficial lamina in *Runx1*$^{-/-}$ mice (R, red).

afferents. The Ret$^+$ to TrkA$^+$ cell-fate transition is, however, incomplete because IB4 labeling and expression of SP, markers for Ret$^+$ and TrkA$^+$ neurons, respectively, either persist or only show a modest expansion. Runx1 is therefore a major, albeit not the sole, determinant of Ret$^+$ nociceptor cell fate. Our studies suggest that peptidergic nociceptors may represent a ground differentiation state, established in the absence of Runx1. In *C. elegans*, mutations in several transcription factors causes a partial transformation of diverse types of sensory neurons into a "default" chemosensory neuron fate (Lanjuin and Sengupta, 2004), suggesting that some of the logic governing sensory neuron diversification has been conserved during evolution.

Runx1 is initially expressed broadly in embryonic nociceptor neurons, but its expression is extinguished selectively in adult TrkA$^+$ neurons. The ability of Runx1 in suppressing many features associated with TrkA$^+$ neurons explains the necessity for its downregulation. However, it should be pointed out that *TRPA1*, expression of

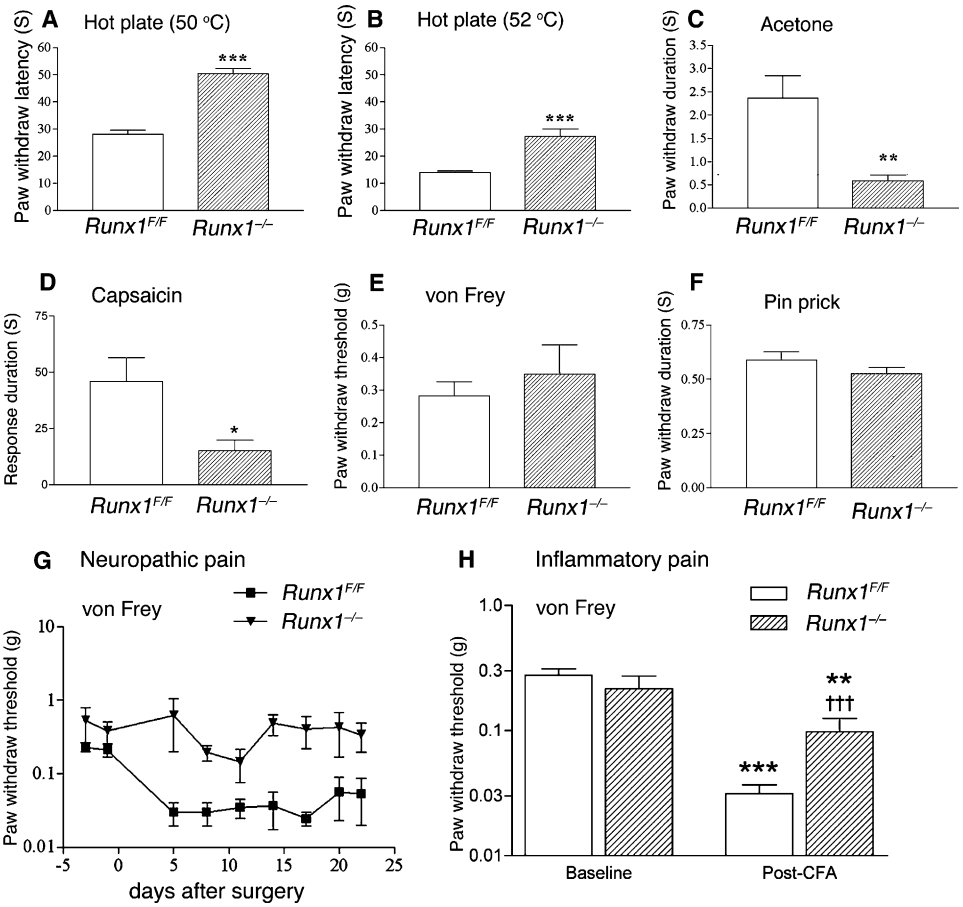

Figure 8. Pain Behavioral Deficits in *Runx1* Mutant Mice

(A–F) Behavioral sensitivity of control *Runx1*$^{F/F}$ mice (open bars) and *Runx1*$^{-/-}$ mice (hatched bars) in tests of heat (hotplate) (A and B), cold (acetone evaporation) (C), Capsaicin-mediated (D), and mechanical pain measured with Von Frey hair (E) or pinprick stimuli (F). For (A)–(C), (E), and (F), n = 19 for control *Runx1*$^{F/F}$, and n = 16 for mutant groups. For (D), n = 7 for both control *Runx1*$^{F/F}$ and mutant groups. Asterisk $p < 0.05$, double asterisk $p < 0.01$, and triple asterisk $p < 0.001$.

(G and H) Mechanical allodynia in control *Runx1*$^{F/F}$ and *Runx1*$^{-/-}$ mice in the spared nerve injury (SNI) model of neuropathic pain and (H) intraplantar complete Freund's adjuvant (CFA) model of inflammatory pain. n = 6 each group for SNI (G), and n = 13 control *Runx1*$^{F/F}$ mice, and n = 10 *Runx1*$^{-/-}$ groups for CFA (H). All data in (A)–(F) and (H) are presented as average (± SEM). Error bars in (G) show the actual range of the data. Double asterisk $p < 0.01$ and triple asterisk $p < 0.001$ compared to baseline and triple dagger $p < 0.001$ to control *Runx1*$^{F/F}$ mice.

which is eliminated in *Runx1*$^{-/-}$ mice, is associated exclusively with peptidergic, and thus presumably TrkA^{+}, neurons (Story et al., 2003). Therefore, although persistent Runx1 expression promotes a Ret^{+} over a TrkA^{+} cell fate, its transient expression in peptidergic neurons also plays a role for the specification of certain transduction phenotypes.

Coordinated Regulation of Nociceptive Transduction Phenotypes

Our data suggest that specificity of expression of nociceptive ion channels/receptors in distinct nociceptors is subject to coordinated transcriptional control. First, *Runx1* is required to activate and to suppress separate groups of ion channels and receptors (Figure 5E). Second, many *Runx1*-dependent channels, including TRP thermal channels and Mrgpr class GPCRs, are expressed in a partially overlapping or nonoverlapping fashion (Dong et al., 2001; Lembo et al., 2002; Story et al., 2003; Woodbury et al., 2004; Zylka et al., 2003, 2005). Third, a recent genome-scale screen of transcription factors (TFs) expressed in the nervous system (Gray et al., 2004) so far fails to identify TFs that are expressed in a subset of IB4^{+};Runx1^{+} neurons (C.-L.C. and Q.M., unpublished data), despite the tremendous diversity of this group of neurons (Dong et al., 2001; Zylka et al., 2003), implying that determination of nociceptor phenotype might be controlled by a limited number of TFs.

Coordinated regulation of diverse sensory channels/receptors appears to be a common theme. In the mammalian olfactory system, each olfactory neuron expresses one of a 1,000 olfactory receptors (ORs) (Mombaerts, 2004; Shykind, 2005). Recent genetic studies, however, demonstrate that each olfactory neuron is competent to activate any of several hundred ORs expressed in the same zone of the olfactory nasal epithelium, implying a coordinated but somehow stochastic control mechanism (Lewcock and Reed, 2004; Serizawa et al., 2003; Shykind et al., 2004). Transcription factors responsible for OR expression, however, have not been characterized. Therefore, the demonstration that *Runx1* is required for the expression of many nonoverlapping

nociceptive ion channels/receptors provides an important steppingstone to unravelling the logic behind sensory neuron diversity.

Coordination between the Specification of Sensory Modality and Central Target Selection

In Ret$^+$;IB4$^+$ nociceptors, Runx1 controls both the expression of nociceptive ion channels (Figures 4–6) and central afferent target selection (Figure 7). A requirement for afferent target selection, but not initial axon pathfinding, appears to be an evolutionally conserved function for Runt domain proteins. In *Runx3*$^{-/-}$ mice, muscle afferents enter the spinal cord but fail to reach their targets in the ventral horn and in the intermediate spinal cord (Inoue et al., 2002; Levanon et al., 2002). In the *Drosophila* visual system, the Runt protein Run is expressed in R7 and R8 photoreceptors that innervate the distal layer (the medulla) in the optic lobe, whereas R1–R6 photoreceptors that lack Run innervate the proximal layer (the lamina) (Kaminker et al., 2002). Ectopic expression of Run in R2 and R6 is sufficient to cause these neurons to switch their projections from the lamina to the medulla (Kaminker et al., 2002).

How might Runx1 coordinate sensory modality specification and afferent target selection? In the olfactory system, axon targeting involves olfactory receptors (Reed, 2004). However, available genetic data do not suggest that nociceptor ion channels or receptors are required for central target selections (Caterina et al., 2000; Zylka et al., 2005). One possibility, therefore, is that Runx1 may also control the expression of molecules responsible for afferent target selection. In this regard, it is noteworthy that at embryonic stages, CGRP expression is associated exclusively with neurons that express low or negligible levels of Runx1 (Figure 5; data not shown), and CGRP$^+$ afferents project to the most superficial lamina. Furthermore, in the absence of *Runx1*, IB4$^+$ afferents switch their projections from lamina IIi to the most superficial lamina. These data suggest that a low level of Runx1 in nociceptive sensory neurons may confer a proximal laminar projection, whereas high levels of Runx1 may confer distal projections.

Association of a Runx1-Mediated Differentiation Program with Specific Pain Behaviors

Runx1 function is required specifically for thermal and neuropathic pain but not for mechanical pain. The pain defect in *Runx1*$^{-/-}$ mice could be caused by loss of expression of nociceptive ion channels, alterations in central connectivity, or both. Despite this complexity, TRP channels have been implicated in noxious cold and heat pain sensitivity (Jordt et al., 2003; Wang and Woolf, 2005), and their loss or reduction likely contributes to the heat and cold pain deficits observed in *Runx1*$^{-/-}$ mice. The loss of a high level of *TRPV1* expression might also contribute to the deficit of capsaicin-induced pain. The prominent roles of Runx1 for the development of Ret$^+$ nociceptors and the dramatic loss of neuropathic pain in *Runx1*$^{-/-}$ mice are consistent with previous findings that the GDNF family of neurotrophins, which signals through Ret, has a therapeutic effect on neuropathic pain (Boucher et al., 2000; Gardell et al., 2003; Malmberg et al., 1997; McMahon and Jones, 2004; Snider and McMahon, 1998), although we can not rule out that a defect in peptidergic neurons, as implicated by the loss of *TRPA1*, may contribute to the behavioral phenotypes.

The normal response of *Runx1*$^{-/-}$ mice to noxious mechanical stimuli implies that *Runx1*-independent ion channels could serve as the candidates for still elusive noxious mechanic transducers. The absence of *TRPA1* expression in *Runx1*$^{-/-}$ mice rules out that TRPA1 functions as an exclusive mechanotransducer in nociceptors, even though it has a role in mechanotransduction in the vestibular apparatus and cochlea (Corey et al., 2004; Nagata et al., 2005). Genetic ablation of *DRASIC* results in a reduction of mechanosensitivity in nociceptors, but *DRASIC* mutant mice do not show obvious mechanical pain deficits (Price et al., 2001). However, it remains a formal possibility that the derepression of *DRASIC* in *Runx1*$^{-/-}$ mice may confer some nociceptors a new capacity to mediate noxious mechanical stimuli.

Analogous Functions of Runx Proteins in Controlling Nociceptor and T Cell Development

In the immune system, Runx proteins segregate two major classes of T cells, CD4$^+$ and CD8$^+$, by suppressing CD4 and activating CD8 expression (de Bruijn and Speck, 2004; Taniuchi and Littman, 2004; Taniuchi et al., 2002). This is, in many ways, analogous to the role of Runx1 in controlling the segregation of TrkA$^+$ and Ret$^+$ nociceptors: suppressing TrkA and activating Ret. In addition, Runx1 is required for the expression of a variety of T cell receptors, including the rearrangement/expression of TCR-β and the subsequent emergence of the T cell diversity (de Bruijn and Speck, 2004; Taniuchi and Littman, 2004; Taniuchi et al., 2002). Runx1 is therefore associated with the generation of the diversity of cells that respond to noxious stimuli or pathogen infection, two innate defense systems that have evolved to enhance animal survival.

Conclusion

Mammalian nociceptive sensory neurons process an diverse range of peripheral noxious stimuli, a repertoire endowed by virtue of their expression of distinct ion channels and receptors that serve as selective sensory transducers. In principle, the specialized sensory modalities of individual classes of nociceptive sensory neurons could be established independently and in piecemeal fashion. Our data, however, provide strong evidence that Runx1 is required to specify the receptive properties of a large cohort of nociceptive sensory neurons. Furthermore, the dual functions of Runx1 in controlling sensory modality specification and afferent central target selection form a genetic basis for the assembly of specific neural circuits for nociceptive information processing. Finally, the identification of a core transcriptional control program for many of the ion channels and receptors known to transduce noxious stimuli has intriguing implications for the design of more effective pain therapies.

Experimental Procedures

Animals

The generation of *Runx1* conditional mutant and *Wnt1-cre* transgenic mice has been described previously (Growney et al., 2005;

Jiang et al., 2000). The morning that vaginal plugs were observed was considered as E0.5. PCR-based genotyping was performed with the following primers: for Wnt1-Cre allele, 5′-TAT CTC ACG TAC TGA CGG TG-3′ and 5′-CTA GTC TAG ACT AAT CGC CAT CTT CCA GC-3′; for Runx1 wild-type and floxed alleles, 5′-GAG TCC CAG CTG TCA ATT CC-3′ and 5′-GGT GAT GGT CAG AGT GAA GC-3′, with floxed allele showing a larger size of DNA band after gel electrophoresis.

In Situ Hybridization and Immunostaining

Detailed protocols for section in situ hybridization are available upon request. The following mouse in situ probes, *TRPA1* (0.9 kb), *TRPM8* (0.71 kb), *TRPV1* (0.72 kb), *TrkA* (0.7 kb), *TRPV2* (0.8kb), *DRASIC* (1.0kb), *P2X3*(1.1kb), *TRPC3* (0.8kb), and *Nav1.9* were amplified with gene-specific sets of PCR primers and cDNA templates prepared from P0 mouse DRG. For immunostaining on frozen sections, the embryos were collected in ice-cold PBS, fixed in 4% paraformaldehyde in PBS, and saturated with 20% sucrose in PBS overnight at 4ºC. For adult mice, after perfused with 4% paraformaldehyde in PBS, dorsal root ganglia were dissected and collected in 4% paraformaldehyde for 1 hr and saturated with 20% sucrose in PBS overnight at 4ºC. Adjacent sections of 14 μm thickness were blocked with 1%BSA plus 0.1% Triton in PBS for 1 hr and incubated at 4ºC overnight with the following cell-type-specific antibodies: rabbit or guinea pig anti-Runx1 (T. Jessell, Columbia University), IB4-Biotin (10 μg/ml, Sigma), and Rabbit TrkA (L. Reichardt, UCSF). Runx1 antibody (1:4000) was against the peptide sequence GRASGMTSL SAELSSRL and prepared in Jessell lab. The specificity of Runx1 antibody was confirmed by the matching of its normal expression and the elimination of its staining in *Runx1*$^{-/-}$ DRG. The primary antibodies were detected with species-specific fluorescence-conjugated secondary antibodies.

For in situ hybridization combined with Runx1 fluorescent immunostaining or IB4 staining, in situ hybridization was first performed without proteinase K treatment, followed by immunostaining with Runx1 antibody or by incubation with fluorescence-conjugated IB4. The in situ signals were photographed under transluminescent light and converted into pseudo-red fluorescent color, whereas Runx1 protein was detected with Alexa 488-conjugated secondary antibodies (Molecular Probes).

For double staining of *TRPM8* mRNA and Ret protein (Figure 6), in situ hybridization with digoxenin (dig)-labeled *TRPM8* probe was first performed without proteinase K treatment. The slide sections were blocked in 1% BSA plus 0.1% Triton in PBS for 1 hr, followed by immunostaining with goat anti-Ret antibody (Molecular Probes) and Alexa 488-conjugated secondary antibodies (Molecular Probes). After fluorescent images were acquired under fluorescent microscope, the slide sections were blocked with 10% goat serum, incubated with alkaline phosphatase (AP)-conjugated goat anti-dig antibody (Roche), followed by AP reaction with NBT/BCIP substrate to generate purple staining for *TRPM8* mRNA. The in situ signals were then photographed under transluminescent light and converted into pseudo-red fluorescent color. The Ret fluorescent images (green) were then carefully overlaid with *TRPM8* images (red). This reverse procedure allowed double staining with two antibodies made in goats.

Cell Counting

To count total DRG neurons, we dissected L5 DRG from three pairs of *Runx1*$^{-/-}$ and control *Runx1*$^{F/F}$ mice, fixed, and embedded, sectioned with 10 μm thickness, hybridized with the panneural marker *SCG10*, and numbers of *SCG10*$^{+}$ neurons were counted. Only cells containing nuclei were counted. To determine the percentages of neurons expressing molecular markers, we prepared six adjacent sets of sections from each L4 or L5 DRG and probed separately with six different probes, one of which was the panneuronal marker *SCG10* to determine the total number of neurons so that percentages can be calculated. Four to eight independent L4 and L5 DRG were used for each counting. Our counting is different from what most people did. Instead of relying on morphology to identify neurons, we determine the total neuron number by counting cells expressing *SCG10*. Our methods allow us to determine some very small sensory neurons. The in situ hybridization methods also led us to identify *Ret*$^{+}$ neurons that expressed at medium/low levels.

Surgery

The spared nerve injury (SNI) model was performed on *Runx1*$^{-/-}$ and control *Runx1*$^{F/F}$ mice as described for rats (Decosterd and Woolf, 2000). Briefly, animals were anesthetized with isoflurane (3% induction, 2% maintenance). An incision was made on the lateral thigh, and the underlying muscle was separated to expose the sciatic nerve. The three terminal branches of the sciatic nerve (tibial, common peroneal, and sural nerves) were carefully separated while minimizing any contact with or stretching of the sural nerve. The tibial and common peroneal nerves were then individually ligated with 6.0 silk and cut distally. 2–3 mm of each nerve distal to the ligation was removed. The muscle incision was closed with silk sutures and the skin with surgical staples. For CFA-mediated inflammation, mice were briefly anesthetized with isoflurane (2–3 min), and 15 μl of complete Freund's adjuvant (CFA) was injected into the plantar surface of the left hindpaw. The thickness of the feet, before and 2 days after CFA injection, were measured to examine inflammatory responses. In five *Runx1*$^{F/F}$ control mice, the thickness of the feet increased from 2.20 ± 0.05 mm to 3.45 ± 0.30 mm (t test, $p < 0.01$), and five *Runx1*$^{-/-}$ Mice show a similar increase, from 2.19 ± 0.08 mm to 3.65 ± 0.12 mm (t test, $p < 0.001$). There is no significant difference in the thickness of CFA-injected feet between *Runx1*$^{F/F}$ control versus *Runx1*$^{-/-}$ mice ($p = 0.11$, with $p < 0.05$ considered as significant).

Behavioral Testing

All animals were acclimatized to the behavioral testing apparatus on at least three "habituation" sessions. After habituation, at least two baseline measures were obtained for each of the behavioral tests on two separate occasions the week before surgery. After the surgical procedures (day 0), the behavioral tests were performed at defined intervals. The tester was blinded to the genotype of each animal. To measure mechanical pain, we placed animals on an elevated wire grid and the lateral plantar surface of the hindpaw stimulated with von Frey monofilaments (0.0174–4.57 g) or pinprick. The withdrawal threshold for the von Frey assay was determined as the filament at which the animal withdrew its paw at least twice in ten applications. The pinprick was measured as duration of time that the animal elevated or licked the paw over a 20 s period immediately after the pinprick. To measure cold pain, we placed animals on an elevated wire grid. A drop of acetone was applied to the plantar hindpaw with a feeding tube attached to a syringe. The duration of time that the animal elevated or licked the paw over a 90 s period immediately after application of the acetone drop was measured. To measure heat pain, we placed mice on a hot plate (Ugo Basile, Italy) and the latency to hindpaw flicking, licking, or jumping measured. The hot plate was set to three difference temperatures, 50ºC, 52ºC, and 55ºC, and all animals were tested sequentially at each temperature with at least 5 min between tests. A cutoff time of 60 s was used for testing at 50ºC. To measure capsaicin-evoked pain, mice were given a 2.5 μg/10 μl intraplantar injection of capsaicin (in 12.5% ethanol) and immediately placed in the behavioral testing apparatus, and the duration of hindpaw licking or raising was measured for a period of 5 min.

Statistical Analyses of Pain Behaviors

Baseline data (and all nonprocedural testing data) was taken as the mean of two tests performed. Post-CFA data was taken from a single test performed 2 days postinjection. Postsurgery behavioral data were analyzed by Student's t test when comparing two groups (Graphpad Prism, Graphpad, San Diego, CA) and two-way repeated measures ANOVA followed by Bonferroni's posttest for time courses of two or more groups (R, v. 1.7.0, R Development Core Team, Vienna, Austria). Log data was used for statistical analysis of von Frey results. $p < 0.05$ was accepted as statistical significance.

Acknowledgments

We thank Nancy Speck and Gary Gilliland for *Runx1* conditional knockout mice, David Rowitch and Andrew McMahon for *Wnt1-Cre* transgenic mice, Robert Griffin for help with statistical analyses of the behavioral data, and Louis Reichardt for the anti-TrkA antibody. We thank Nancy Speck, Gary Gilliland, Chuck Stiles, Michael Greenberg, and Silvia Arber for comments on the manuscript. The

work is supported by grants from the National Institutes of Health to Q.M. and C.J.W. C.C. is a fellow of Charles King Medical foundation, J.C.D. is a fellow of Helen Hay Whitney Foundation, Q.M. is a Claudia Adams Barr Scholar and a Pew Scholar in Biomedical Sciences, and T.M.J. is an investigator of the Howard Hughes Medical Institute.

Received: May 11, 2005
Revised: October 11, 2005
Accepted: October 25, 2005
Published: February 1, 2006

References

Agarwal, N., Offermanns, S., and Kuner, R. (2004). Conditional gene deletion in primary nociceptive neurons of trigeminal ganglia and dorsal root ganglia. Genesis *38*, 122–129.

Boucher, T.J., Okuse, K., Bennett, D.L., Munson, J.B., Wood, J.N., and McMahon, S.B. (2000). Potent analgesic effects of GDNF in neuropathic pain states. Science *290*, 124–127.

Bradbury, E.J., Burnstock, G., and McMahon, S.B. (1998). The expression of P2X3 purinoreceptors in sensory neurons: effects of axotomy and glial-derived neurotrophic factor. Mol. Cell. Neurosci. *12*, 256–268.

Caterina, M.J., Schumacher, M.A., Tominaga, M., Rosen, T.A., Levine, J.D., and Julius, D. (1997). The capsaicin receptor: a heat-activated ion channel in the pain pathway. Nature *389*, 816–824.

Caterina, M.J., Leffler, A., Malmberg, A.B., Martin, W.J., Trafton, J., Petersen-Zeitz, K.R., Koltzenburg, M., Basbaum, A.I., and Julius, D. (2000). Impaired nociception and pain sensation in mice lacking the capsaicin receptor. Science *288*, 306–313.

Chen, C.C., Akopian, A.N., Sivilotti, L., Colquhoun, D., Burnstock, G., and Wood, J.N. (1995). A P2X purinoceptor expressed by a subset of sensory neurons. Nature *377*, 428–431.

Corey, D.P., Garcia-Anoveros, J., Holt, J.R., Kwan, K.Y., Lin, S.Y., Vollrath, M.A., Amalfitano, A., Cheung, E.L., Derfler, B.H., Duggan, A., et al. (2004). TRPA1 is a candidate for the mechanosensitive transduction channel of vertebrate hair cells. Nature *432*, 723–730.

Craig, A.D. (2003). Pain mechanisms: labeled lines versus convergence in central processing. Annu. Rev. Neurosci. *26*, 1–30.

de Bruijn, M.F., and Speck, N.A. (2004). Core-binding factors in hematopoiesis and immune function. Oncogene *23*, 4238–4248.

Decosterd, I., and Woolf, C.J. (2000). Spared nerve injury: an animal model of persistent peripheral neuropathic pain. Pain *87*, 149–158.

Dib-Hajj, S.D., Tyrrell, L., Black, J.A., and Waxman, S.G. (1998). NaN, a novel voltage-gated Na channel, is expressed preferentially in peripheral sensory neurons and down-regulated after axotomy. Proc. Natl. Acad. Sci. USA *95*, 8963–8968.

Dong, X., Han, S., Zylka, M.J., Simon, M.I., and Anderson, D.J. (2001). A diverse family of GPCRs expressed in specific subsets of nociceptive sensory neurons. Cell *106*, 619–632.

Eng, S.R., Lanier, J., Fedtsova, N., and Turner, E.E. (2004). Coordinated regulation of gene expression by Brn3a in developing sensory ganglia. Development *131*, 3859–3870.

Gardell, L.R., Wang, R., Ehrenfels, C., Ossipov, M.H., Rossomando, A.J., Miller, S., Buckley, C., Cai, A.K., Tse, A., Foley, S.F., et al. (2003). Multiple actions of systemic artemin in experimental neuropathy. Nat. Med. *9*, 1383–1389.

Gray, P.A., Fu, H., Luo, P., Zhao, Q., Yu, J., Ferrari, A., Tenzen, T., Yuk, D.I., Tsung, E.F., Cai, Z., et al. (2004). Mouse brain organization revealed through direct genome-scale TF expression analysis. Science *306*, 2255–2257.

Grazzini, E., Puma, C., Roy, M.O., Yu, X.H., O'Donnell, D., Schmidt, R., Dautrey, S., Ducharme, J., Perkins, M., Panetta, R., et al. (2004). Sensory neuron-specific receptor activation elicits central and peripheral nociceptive effects in rats. Proc. Natl. Acad. Sci. USA *101*, 7175–7180.

Growney, J.D., Shigematsu, H., Li, Z., Lee, B.H., Adelsperger, J., Rowan, R., Curley, D.P., Kutok, J.L., Akashi, K., Williams, I.R., et al. (2005). Loss of Runx1 perturbs adult hematopoiesis and is associated with a myeloproliferative phenotype. Blood *106*, 494–504.

Huang, E.J., and Reichardt, L.F. (2001). Neurotrophins: roles in neuronal development and function. Annu. Rev. Neurosci. *24*, 677–736.

Hunt, S.P., and Mantyh, P.W. (2001). The molecular dynamics of pain control. Nat. Rev. Neurosci. *2*, 83–91.

Inoue, K., Ozaki, S., Shiga, T., Ito, K., Masuda, T., Okado, N., Iseda, T., Kawaguchi, S., Ogawa, M., Bae, S.C., et al. (2002). Runx3 controls the axonal projection of proprioceptive dorsal root ganglion neurons. Nat. Neurosci. *5*, 946–954.

Jiang, X., Rowitch, D.H., Soriano, P., McMahon, A.P., and Sucov, H.M. (2000). Fate of the mammalian cardiac neural crest. Development *127*, 1607–1616.

Jordt, S.E., McKemy, D.D., and Julius, D. (2003). Lessons from peppers and peppermint: the molecular logic of thermosensation. Curr. Opin. Neurobiol. *13*, 487–492.

Julius, D., and Basbaum, A.I. (2001). Molecular mechanisms of nociception. Nature *413*, 203–210.

Kaminker, J.S., Canon, J., Salecker, I., and Banerjee, U. (2002). Control of photoreceptor axon target choice by transcriptional repression of Runt. Nat. Neurosci. *5*, 746–750.

Komori, T. (2005). Regulation of skeletal development by the Runx family of transcription factors. J. Cell. Biochem. *95*, 445–453.

Lanjuin, A., and Sengupta, P. (2004). Specification of chemosensory neuron subtype identities in *Caenorhabditis elegans*. Curr. Opin. Neurobiol. *14*, 22–30.

Lei, L., Laub, F., Lush, M., Romero, M., Zhou, J., Luikart, B., Klesse, L., Ramirez, F., and Parada, L.F. (2005). The zinc finger transcription factor Klf7 is required for TrkA gene expression and development of nociceptive sensory neurons. Genes Dev. *19*, 1354–1364.

Lembo, P.M., Grazzini, E., Groblewski, T., O'Donnell, D., Roy, M.O., Zhang, J., Hoffert, C., Cao, J., Schmidt, R., Pelletier, M., et al. (2002). Proenkephalin A gene products activate a new family of sensory neuron-specific GPCRs. Nat. Neurosci. *5*, 201–209.

Levanon, D., Bettoun, D., Harris-Cerruti, C., Woolf, E., Negreanu, V., Eilam, R., Bernstein, Y., Goldenberg, D., Xiao, C., Fliegauf, M., et al. (2002). The Runx3 transcription factor regulates development and survival of TrkC dorsal root ganglia neurons. EMBO J. *21*, 3454–3463.

Lewcock, J.W., and Reed, R.R. (2004). A feedback mechanism regulates monoallelic odorant receptor expression. Proc. Natl. Acad. Sci. USA *101*, 1069–1074.

Lewin, G.R., and Moshourab, R. (2004). Mechanosensation and pain. J. Neurobiol. *62*, 30–44.

Lewin, G.R., Lu, Y., and Park, T.J. (2004). A plethora of painful molecules. Curr. Opin. Neurobiol. *14*, 443–449.

Li, J.L., Ding, Y.Q., Li, Y.Q., Li, J.S., Nomura, S., Kaneko, T., and Mizuno, N. (1998). Immunocytochemical localization of mu-opioid receptor in primary afferent neurons containing substance P or calcitonin gene-related peptide. A light and electron microscope study in the rat. Brain Res. *794*, 347–352.

Light, A.R., and Perl, E.R. (1979a). Reexamination of the dorsal root projection to the spinal dorsal horn including observations on the differential termination of coarse and fine fibers. J. Comp. Neurol. *186*, 117–131.

Light, A.R., and Perl, E.R. (1979b). Spinal termination of functionally identified primary afferent neurons with slowly conducting myelinated fibers. J. Comp. Neurol. *186*, 133–150.

Ma, Q., Fode, C., Guillemot, F., and Anderson, D.J. (1999). NEUROGENIN1 and NEUROGENIN2 control two distinct waves of neurogenesis in developing dorsal root ganglia. Genes Dev. *13*, 1717–1728.

Ma, L., Lei, L., Eng, S.R., Turner, E., and Parada, L.F. (2003). Brn3a regulation of TrkA/NGF receptor expression in developing sensory neurons. Development *130*, 3525–3534.

Malmberg, A.B., Chen, C., Tonegawa, S., and Basbaum, A.I. (1997). Preserved acute pain and reduced neuropathic pain in mice lacking PKCgamma. Science *278*, 279–283.

Marchand, F., Perretti, M., and McMahon, S.B. (2005). Role of the immune system in chronic pain. Nat. Rev. Neurosci. *6*, 521–532.

McEvilly, R.J., Erkman, L., Luo, L., Sawchenko, P.E., Ryan, A.F., and Rosenfeld, M.G. (1996). Requirement for Brn-3.0 in differentiation and survival of sensory and motor-neurons. Nature *384*, 574–577.

McKemy, D.D., Neuhausser, W.M., and Julius, D. (2002). Identification of a cold receptor reveals a general role for TRP channels in thermosensation. Nature *416*, 52–58.

McMahon, S.B., and Jones, N.G. (2004). Plasticity of pain signaling: role of neurotrophic factors exemplified by acid-induced pain. J. Neurobiol. *61*, 72–87.

Molliver, D.C., Wright, D.E., Leitner, M.L., Parsadanian, A.S., Doster, K., Wen, D., Yan, Q., and Snider, W.D. (1997). IB4-binding DRG neurons switch from NGF to GDNF dependence in early postnatal life. Neuron *19*, 849–861.

Mombaerts, P. (2004). Odorant receptor gene choice in olfactory sensory neurons: the one receptor-one neuron hypothesis revisited. Curr. Opin. Neurobiol. *14*, 31–36.

Nagata, K., Duggan, A., Kumar, G., and Garcia-Anoveros, J. (2005). Nociceptor and hair cell transducer properties of TRPA1, a channel for pain and hearing. J. Neurosci. *25*, 4052–4061.

Patapoutian, A., Peier, A.M., Story, G.M., and Viswanath, V. (2003). ThermoTRP channels and beyond: mechanisms of temperature sensation. Nat. Rev. Neurosci. *4*, 529–539.

Peier, A.M., Moqrich, A., Hergarden, A.C., Reeve, A.J., Andersson, D.A., Story, G.M., Earley, T.J., Dragoni, I., McIntyre, P., Bevan, S., and Patapoutian, A. (2002). A TRP channel that senses cold stimuli and menthol. Cell *108*, 705–715.

Perl, E.R. (1984). Pain and nociception. In Handbook of Physiology: The Nervous System, I. Darian-Smith, ed. (Bethesda, MD: American Physiology Society), pp. 915–975.

Perl, E.R. (1998). Getting a line on pain: is it mediated by dedicated pathways? Nat. Neurosci. *1*, 177–178.

Potrebic, S., Ahn, A.H., Skinner, K., Fields, H.L., and Basbaum, A.I. (2003). Peptidergic nociceptors of both trigeminal and dorsal root ganglia express serotonin 1D receptors: implications for the selective antimigraine action of triptans. J. Neurosci. *23*, 10988–10997.

Price, M.P., McIlwrath, S.L., Xie, J., Cheng, C., Qiao, J., Tarr, D.E., Sluka, K.A., Brennan, T.J., Lewin, G.R., and Welsh, M.J. (2001). The DRASIC cation channel contributes to the detection of cutaneous touch and acid stimuli in mice. Neuron *32*, 1071–1083.

Price, D.D., Greenspan, J.D., and Dubner, R. (2003). Neurons involved in the exteroceptive function of pain. Pain *106*, 215–219.

Reed, R.R. (2004). After the holy grail: establishing a molecular basis for Mammalian olfaction. Cell *116*, 329–336.

Scholz, J., and Woolf, C.J. (2002). Can we conquer pain? Nat. Neurosci. *5* (*Suppl*), 1062–1067.

Serizawa, S., Miyamichi, K., Nakatani, H., Suzuki, M., Saito, M., Yoshihara, Y., and Sakano, H. (2003). Negative feedback regulation ensures the one receptor-one olfactory neuron rule in mouse. Science *302*, 2088–2094.

Shykind, B.M. (2005). Regulation of odorant receptors: one allele at a time. Hum. Mol. Genet. *14*, 33–39.

Shykind, B.M., Rohani, S.C., O'Donnell, S., Nemes, A., Mendelsohn, M., Sun, Y., Axel, R., and Barnea, G. (2004). Gene switching and the stability of odorant receptor gene choice. Cell *117*, 801–815.

Snider, W.D., and McMahon, S.B. (1998). Tackling pain at the source: new ideas about nociceptors. Neuron *20*, 629–632.

Stein, G.S., Lian, J.B., van Wijnen, A.J., Stein, J.L., Montecino, M., Javed, A., Zaidi, S.K., Young, D.W., Choi, J.Y., and Pockwinse, S.M. (2004). Runx2/Cbfa1: a multifunctional regulator of bone formation. Oncogene *23*, 4315–4329.

Story, G.M., Peier, A.M., Reeve, A.J., Eid, S.R., Mosbacher, J., Hricik, T.R., Earley, T.J., Hergarden, A.C., Andersson, D.A., Hwang, S.W., et al. (2003). ANKTM1, a TRP-like channel expressed in nociceptive neurons, is activated by cold temperatures. Cell *112*, 819–829.

Taniuchi, I., and Littman, D.R. (2004). Epigenetic gene silencing by Runx proteins. Oncogene *24*, 4341–4345.

Taniuchi, I., Osato, M., Egawa, T., Sunshine, M.J., Bae, S.C., Komori, T., Ito, Y., and Littman, D.R. (2002). Differential requirements for Runx proteins in CD4 repression and epigenetic silencing during T lymphocyte development. Cell *111*, 621–633.

Theriault, F.M., Roy, P., and Stifani, S. (2004). *AML1/Runx1* is important for the development of hindbrain cholinergic branchiovisceral motor neurons and selected cranial sensory neurons. Proc. Natl. Acad. Sci. USA *101*, 10343–10348.

Tominaga, M., and Caterina, M.J. (2004). Thermosensation and pain. J. Neurobiol. *61*, 3–12.

Waldmann, R., and Lazdunski, M. (1998). H(+)-gated cation channels: neuronal acid sensors in the NaC/DEG family of ion channels. Curr. Opin. Neurobiol. *8*, 418–424.

Wang, H., and Woolf, C.J. (2005). Pain TRPs. Neuron *46*, 9–12.

Wood, J.N. (2004). Recent advances in understanding molecular mechanisms of primary afferent activation. Gut Suppl *53*, ii9–ii12.

Wood, J.N., Boorman, J.P., Okuse, K., and Baker, M.D. (2004). Voltage-gated sodium channels and pain pathways. J. Neurobiol. *61*, 55–71.

Woodbury, C.J., Zwick, M., Wang, S., Lawson, J.J., Caterina, M.J., Koltzenburg, M., Alberts, K.M., Koerber, H.R., and David, B.M. (2004). Nociceptors lacking TRPV1 and TRPV2 have normal heat responses. J. Neurosci. *24*, 6410–6415.

Woolf, C. (2004). Dissecting out mechanisms responsible for peripheral neuropathic pain: Implications for diagnosis and therapy. Life Sci. *74*, 2605–2610.

Zylka, M.J., Dong, X., Southwell, A.L., and Anderson, D.J. (2003). Atypical expansion in mice of the sensory neuron-specific Mrg G protein-coupled receptor family. Proc. Natl. Acad. Sci. USA *100*, 10043–10048.

Zylka, M.J., Rice, F.L., and Anderson, D.J. (2005). Topographically distinct epidermal nociceptive circuits revealed by axonal tracers targeted to mrgprd. Neuron *45*, 17–25.